Appendix A
Background of the Bree Diagram

A.1 BASIC BREE DIAGRAM DERIVATION

The Bree diagram (Fig. A.1) is constructed for the purpose of combining mechanical and thermal stresses in a cylindrical shell in order to establish allowable stress criteria. The diagram is plotted with the mechanical stress as an abscissa and the thermal stress as an ordinate. Zones E, S_1, S_2, P, R_1, and R_2, shown in the figure, correspond to specific mechanical and thermal load groupings. The criteria used to establish each of these zones are described below and are based on Bree (1967 and 1968), Burgreen (1975), Kraus (1980), and Wilshire (1983).

Zone E

It is assumed that all stresses in zone E remain elastic in the first half (thermal loading) as well as the second half (thermal down loading) of the thermal cycle. Bree assumed a thin cylindrical shell subjected to internal pressure. The average stresses in the cylinder are

$$\sigma_\theta = PR_i/t \tag{A.1}$$

$$\sigma_\ell = PR_i/2t \tag{A.2}$$

$$\sigma_r = -P, \text{ maximum at the inner surface} \tag{A.3}$$

where

P = internal pressure
R_i = inside radius
t = thickness of cylinder
σ_ℓ = longitudinal stress
σ_r = radial stress
σ_θ = circumferential stress

Radial thermal gradients in thin-walled cylinder are normally linear in distribution. For a linear radial thermal distribution through the thickness (Fig. A.2), the thermal stress equations (Burgreen, 1975) are expressed as

$$\sigma_\theta = \sigma_\ell = (2x/t)\{E\alpha\Delta T/[2(1-\mu)]\} \tag{A.4}$$

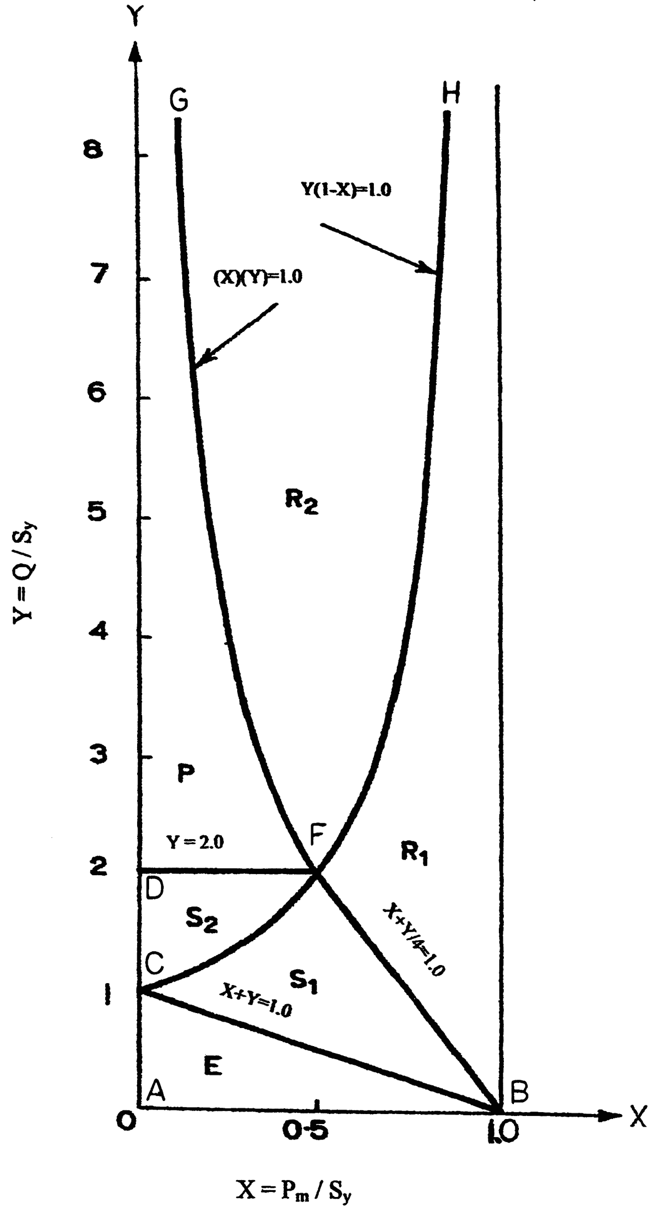

FIG. A.1
BREE DIAGRAM (BREE, 1967)

$$\sigma_r \approx 0 \tag{A.5}$$

where

E = modulus of elasticity
x = distance from midwall of the cylinder (Fig. A.2)
α = coefficient of thermal expansion
ΔT = difference in temperature between inside and outside surfaces of the cylinder
μ = Poisson's ratio

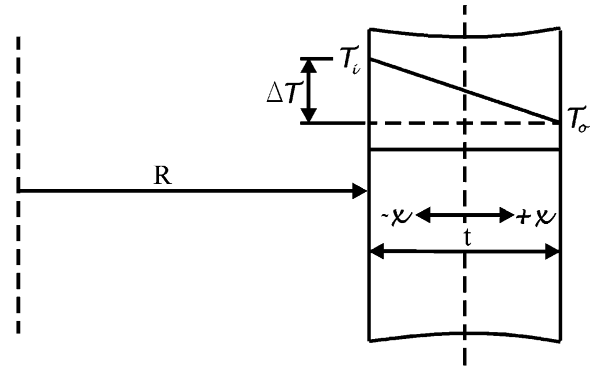

FIG. A.2
THERMAL GRADIENT IN SHELL

Bree made the following assumptions in order to evaluate the mechanical and thermal stress equations in a practical manner:

- Radial mechanical and thermal stresses, σ_r, are small compared to the circumferential and longitudinal stresses and can thus be ignored.
- Because mechanical stress is considered primary stress, it cannot exceed the yield stress value of the material. Radial thermal stress, on the other hand, is considered secondary stress and can thus exceed the yield stress of the material.
- The combination of mechanical and thermal stresses in the θ and ℓ directions may result in stresses past the yield stress in one direction and not the other. Such a condition prevents the formulation of a closed-form solution in a cylindrical shell. Accordingly, Bree made a conservative assumption by setting the stress in the ℓ direction, σ_ℓ, equal to zero.
- With the ℓ and r stresses set to zero, Bree assumed for simplicity that the remaining stress in the θ direction could be applied on a flat plate as shown in Fig. A.3 with σ values obtained from Eqs. (A.1) and (A.4) for cylindrical shells.
- An additional assumption was made where the flat plate is not allowed to rotate due to variable thermal stress across the thickness in order to simulate the actual condition in a cylindrical shell.

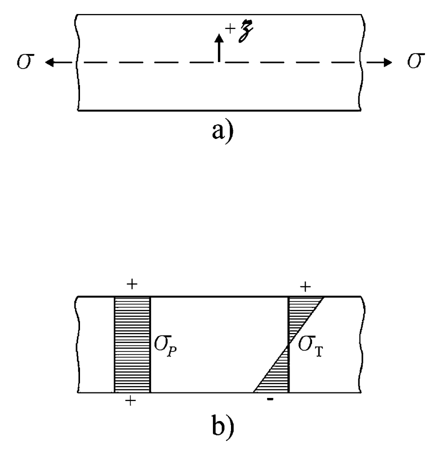

FIG. A.3
STRESS IN THE CIRCUMFERENTIAL DIRECTION

- It is assumed that the material has an elastic perfectly plastic stress-strain diagram.
- The initial evaluation of the mechanical and thermal stresses in the elastic and plastic region was made without any consideration to relaxation or creep.
- The final results were subsequently evaluated for relaxation and creep effect.
- It is assumed that stress due to pressure is held constant, whereas thermal stress is cycled. Hence, pressure and temperature stress exist at the end of the first half of the cycle, and only pressure exists at the end of the second half of the cycle.

Based on these assumptions, the mechanical and thermal stress in zone E can now be derived. It is assumed that the stresses remain elastic during the stress cycle. The stress distribution in the first half-cycle, shown in Fig. A.4, is

$$\sigma = PR_i/t + (2z/t)\{E\alpha\Delta T/[2(1-\mu)]\} \tag{A.6}$$

or

$$\sigma = \sigma_p + (2z/t)\sigma_T \tag{A.7}$$

where

z = distance from midwall of the flat plate (Fig. A.2)
σ_p = stress due to pressure, PR_i/t
σ_T = stress due to temperature, $E\alpha\Delta T/2(1-\mu)$

It should be noted that for a flat plate, Eq. (A.6) uses the quantity $\Delta T/[2(1-\mu)]$ rather than ΔT in order to simulate thermal stress in a cylinder.

The maximum value of Eq. (A.7) is reached when $z = t/2$. In zone E, the stress combination of σ_p plus σ_T is kept below σ_y, as shown in Fig. A.4. Thus, Eq. (A.7) becomes

$$\sigma_p + \sigma_T < \sigma_y \tag{A.8a}$$

Define

$$X = \sigma_p/\sigma_y \qquad \text{and} \qquad Y = \sigma_T/\sigma_y$$

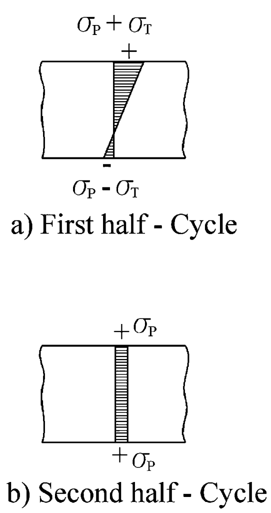

FIG. A.4
STRESS CYCLE IN ZONE E

Then, Eq. (A.8a) becomes

$$X + Y = 1.0 \tag{A.8b}$$

In the second half-cycle, the equation becomes

$$\sigma_p < \sigma_y \tag{A.9}$$

Thus, zone E, which defines an elastic stress condition, is bound by Eq. (A.8) as well as the *x*- and *y*-axes as shown in Fig. A.1.

Zone S_1

In zone S_1, it is assumed that shakedown will occur after the first cycle. It is also assumed that the elastic pressure plus temperature stress combination in the first half-cycle exceeds the yield stress of the material at only one side of the shell, as shown in Fig. A.5. Stress in the second half-cycle after the temperature is removed remains elastic. This assures shakedown after the first cycle. The strain distribution in the elastic region is

$$E\varepsilon_1 = \sigma_1 - (2z/t)\sigma_T \qquad \text{for } -t/2 < z < v \tag{A.10}$$

where the subscript "1" refers to the first half-cycle and *v* is to be determined. The strain distribution in the plastic region is

$$E\varepsilon_1 = \sigma_y - (2z/t)\sigma_T + E\eta \qquad \text{for } v < z < +t/2 \tag{A.11}$$

where η is the plastic component of the stress.

At point *v*, $\sigma_1 = \sigma_y$. Equating Eqs. (A.10) and (A.11) gives

$$E\eta = 2[(z - v)/t]\sigma_T \tag{A.12}$$

And Eqs. (A.10) and (A.11) become

$$\sigma_1 = \sigma_y + 2[(z - v)/t]\sigma_T \qquad \text{in the elastic region} \tag{A.13}$$

$$\sigma_1 = \sigma_y \qquad \text{in the plastic region} \tag{A.14}$$

The expression for *v* is obtained by summing the stress Eqs. (A.13) and (A.14) across the thickness in accordance with the equation

$$\int_{-t/2}^{t/2} \sigma \, dz = t\sigma_p \tag{A.15}$$

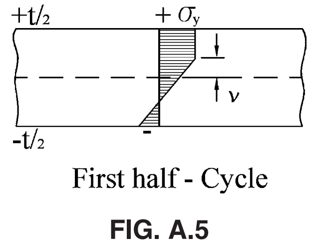

FIG. A.5
STRESS CYCLE IN ZONE S_1 WITH YIELDING ON ONE SIDE ONLY

This gives

$$v/t = [(\sigma_y - \sigma_p)/\sigma_T]^{1/2} - 1/2 \quad \text{(A.16)}$$

A limit of Eq. (A.16) is that v cannot be less than zero. This gives

$$\sigma_p + \sigma_T/4 < \sigma_y \quad \text{(A.17a)}$$

Equation (A.17a) can also be written as

$$X + Y/4 = 1.0 \quad \text{(A.17b)}$$

Another limit of Eq. (A.16) is that v must be less than $t/2$. This gives

$$\sigma_p + \sigma_T < \sigma_y \quad \text{(A.18a)}$$

or

$$X + Y = 1.0 \quad \text{(A.18b)}$$

In order for shakedown to take place, the stresses remaining after removal of the temperature in the second half-cycle must remain elastic. The change of strain from the first to second half-cycle is given by

$$E\Delta\varepsilon_2 = \Delta\sigma_2 + (2z/t)\sigma_T \qquad \text{for } -t/2 < z < v \quad \text{(A.19)}$$

$$= \sigma_2 - \sigma_1 + (2z/t)\sigma_T \quad \text{(A.20)}$$

and

$$E\Delta\varepsilon_2 = \Delta\sigma_2 + (2z/t)\sigma_T \qquad \text{for } v < z < t/2 \quad \text{(A.21)}$$

$$= \sigma_2 - \sigma_y + (2z/t)\sigma_T \quad \text{(A.22)}$$

where the subscript "2" refers to the second half-cycle. Multiplying both sides of Eqs. (A.19) and (A.21) by dz and integrating their total sum results in $\Delta\varepsilon_2 = 0$. This is because the integral of the total sum of $\Delta\sigma_2 = 0$ since there is no change in external forces during the second half-cycle. Also, the total sum of the integral $(2z/t)\sigma_T$ from the limits $-t/2$ to $+t/2$ is equal to zero. Hence,

$$\Delta\varepsilon_2 = 0 \quad \text{(A.23)}$$

Substituting this quantity and Eq. (A.13) into Eqs. (A.20) and (A.22) results in

$$\sigma_2 = \sigma_y - (2v/t)\sigma_T \qquad \text{for } -t/2 < z < v \quad \text{(A.24)}$$

$$\sigma_2 = \sigma_y - (2z/t)\sigma_T \qquad \text{for } v < z < t/2 \quad \text{(A.25)}$$

One of the conditions for shakedown is that $\sigma_2 < \pm\sigma_y$. Hence, the above two equations reduce to

$$v > 0 \quad \text{(A.26)}$$

and

$$\sigma_T < 2\sigma_y \quad \text{(A.27a)}$$

or

$$Y < 2.0 \quad \text{(A.27b)}$$

Thus, zone S_1 is bounded by Eqs. (A.17), (A.18), and (A.27). This is shown by area *BCDF* in Fig. A.1.

Zone S_2

In zone S_2, it is assumed that shakedown will occur after the first cycle. It is also assumed that the elastic pressure plus temperature stress combination in the first half-cycle exceeds the yield stress of the material at both sides of the shell. Stress in the second half-cycle after the temperature is removed remains elastic. This assures shakedown after the first cycle. The derivation of the limiting equations is similar to that in zone S_1 with the exception that both sides of the shell reach the yield stress, as shown in Fig. A.6. Two unknown quantities *v* and *w* must be determined. The solution (Burgreen, 1975) yields

$$v/t = (1/2)[(\sigma_y/\sigma_T) - (\sigma_p/\sigma_y)] \quad \text{(A.28)}$$

$$w/t = -(1/2)[(\sigma_y/\sigma_T) + (\sigma_p/\sigma_y)] \quad \text{(A.29)}$$

A limiting value of these two equations is $v < t/2$ and $w < -t/2$. The two equations reduce to

$$\sigma_T(\sigma_y + \sigma_p) = \sigma_y^2 \quad \text{(A.30)}$$

and

$$\sigma_T\,(\sigma_y - \sigma_p) = \sigma_y^2 \quad \text{(A.31a)}$$

or

$$Y(1 - X) = 1.0 \quad \text{(A.31b)}$$

The second of these equations is the prevalent one, because satisfying it will automatically satisfy the first one. Equation (A.27) is also a controlling equation in the S_2 domain. Thus, Eqs. (A.27) and (A.31) form the boundary of zone S_2. This is shown by area *CDF* in Fig. A.1. Notice that this zone falls within zone S_1. Thus, zone S_2, where yielding occurs on both sides of the shell, supersedes the condition in zone S_1 in the range shown.

Zone P

Plasticity is assumed to occur in zone P. The main characteristics of this zone is that the core section of the shell remains elastic (otherwise, ratcheting may occur) whereas the outer surfaces alternate between tensile and compression yield stress as the temperature is applied then removed as shown in Fig. A.7. Figure A.7a shows the stress distribution at the end of the first half-cycle. It resembles the same figure in the second half-cycle of zone S_2. Figure A.7b shows the stress distribution during the second half-cycle, whereas Fig. A.7c shows the stress distribution at the end of the second half-cycle

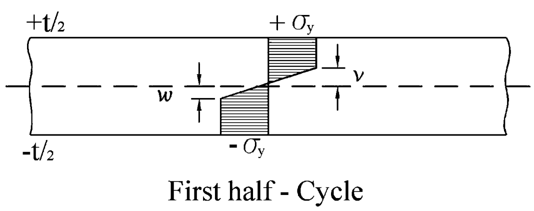

FIG. A.6
STRESS CYCLE IN ZONE S_2 WITH YIELDING ON BOTH SIDES

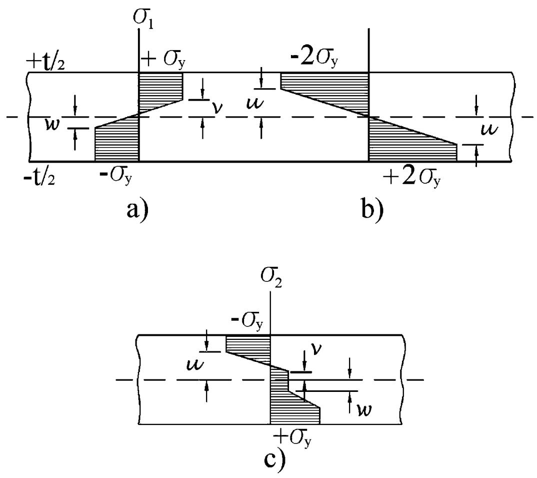

First and Second half - Cycles

FIG. A.7
STRESS CYCLE IN ZONE P

(Burgreen, 1975). Referring to Fig. A.7 with the center portion of the shell remaining elastic, $-u \le z \le u$, the relationship between the stress and strain (Kraus, 1980) is given by

$$E\Delta\varepsilon_2 = \Delta\sigma_2 + (2z/t)\sigma_T \tag{A.32}$$

At the elastic-plastic boundary, the stress increment is $2\sigma_y$ at $z = -u$ and $-2\sigma_y$ at $z = u$. Substituting these two values in Eq. (A.32) and subtracting the resultant two equations, since the strain change is linear, gives

$$u = (\sigma_y/\sigma_T)t \tag{A.33}$$

Because u cannot exceed $t/2$, Eq. (A.33) gives

$$\sigma_T \ge 2\sigma_y \tag{A.34a}$$

or,

$$Y \ge 2 \tag{A.34b}$$

The net stress distribution in the core section of the cylinder (Fig. A.7c) is

$$\sigma = \sigma_y - 2\sigma_T(v/t) \qquad -w \le z \le v \tag{A.35}$$

This stress cannot exceed the yield stress. Thus, Eq. (A.35) gives $v \ge 0$. Substituting this value in Eq. (A.28) gives

$$\sigma_p\sigma_T \le \sigma_y^2 \tag{A.36a}$$

or

$$(X)(Y) = 1 \tag{A.36b}$$

Equations (A.34) and (A.36) form the boundary of zone P. It is defined by area *DFG* of the Bree diagram in Fig. A.1.

Zone R_1

Ratcheting is assumed to take place in zone R_1. The main characteristic of this zone is that yielding extends past the midwall of the shell due to yielding at one of the surfaces of the shell. Thus, shakedown will not take place. Figure A.8 shows the stress distribution in the first and second half-cycles, whereas Fig. A.9 shows the stress distribution in the second and third half-cycles.

The first half-cycle (Fig. A.8a) is the same as the stress distribution in zone S_1. The stress-strain relationship for the second half-cycle (Fig. A.8c) is given by

$$E\Delta\varepsilon_2 = \sigma_y - \sigma_1 + (2z/t)\sigma_T + E\Delta\eta_2 \qquad -t/2 \le z \le v \tag{A.37}$$

$$E\Delta\varepsilon_2 = (2z/t)\sigma_T + E\Delta\eta_2 \qquad v \le z \le v' \tag{A.38}$$

$$E\Delta\varepsilon_2 = \sigma_2 - \sigma_y + (2z/t)\sigma_T \qquad v' \le z \le t/2 \tag{A.39}$$

From Eqs. (A.37), (A.38), and (A.39) plus the boundary conditions shown in Fig. A.8c, the following equations are obtained after various substitutions:

$$\sigma_2 = \sigma_y + 2\sigma_T(v' - z)/t \qquad v' \le z \le t/2 \tag{A.40}$$

$$\sigma_2 = \sigma_y \qquad -t/2 \le z \le v \tag{A.41}$$

$$v'/t = -v/2 = 0.5 - [(\sigma_y - \sigma_p)/\sigma_T)]^{1/2} \tag{A.42}$$

$$E\Delta\eta_2 = 4\sigma_T v'/t \qquad -t/2 \le z \le v \tag{A.43}$$

$$E\Delta\eta_2 = 2\sigma_T\,(v' - z)/t \qquad v \le z \le v' \tag{A.44}$$

In the third half-cycle (Fig. A.9), the temperature stress is re-applied. The stress-strain relationship for the third half-cycle (Fig. A.9c) is given by

$$E\Delta\varepsilon_3 = \sigma_3 - \sigma_y - (2z/t)\sigma_T \qquad -t/2 \le z \le v \tag{A.45}$$

$$E\Delta\varepsilon_3 = -(2z/t)\sigma_T + E\Delta\eta_3 \qquad v \le z \le v' \tag{A.46}$$

$$E\Delta\varepsilon_3 = \sigma_y - \sigma_2 - (2z/t)\sigma_T + E\Delta\eta_3 \qquad v' \le z \le t/2 \tag{A.47}$$

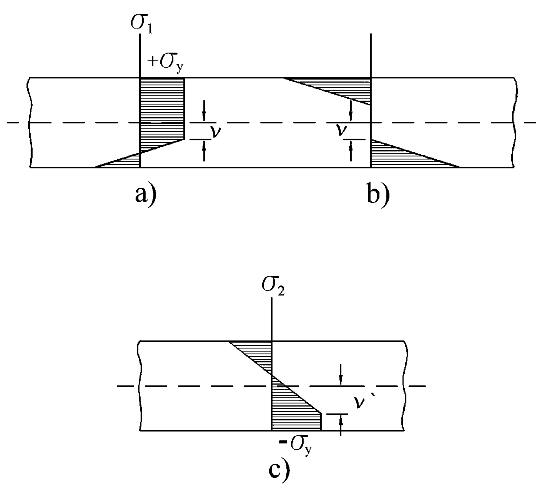

FIG. A.8
FIRST AND SECOND HALF — CYCLES IN ZONE R_1

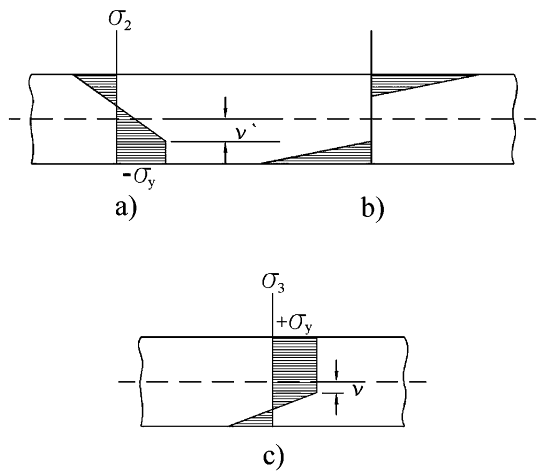

FIG. A.9
SECOND AND THIRD HALF — CYCLES IN ZONE R_1

From Eqs. (A.45), (A.46), and (A.47) plus the boundary conditions shown in Fig. A.9c, the following equations are obtained after various substitutions:

$$\sigma_3 = \sigma_y + 2\sigma_T(z - v)/t \qquad -t/2 \le z \le v \tag{A.48}$$

$$\sigma_3 = \sigma_y \qquad v' \le z \le t/2 \tag{A.49}$$

$$v'/t = -v/2 = 0.5 - [(\sigma_y - \sigma_p)/\sigma_T)]^{1/2} \tag{A.50}$$

$$E\Delta\eta_3 = 2\sigma_T(z - v)/t \qquad v \le z \le v' \tag{A.51}$$

$$E\Delta\eta_3 = 2\sigma_T(v' - v)/t \qquad v' \le z \le t/2 \tag{A.52}$$

The plastic strain through the full cycle is obtained by adding Eqs. (A.44) and (A.52) to obtain

$$E\Delta\eta = 4\sigma_T v'/t \tag{A.53}$$

Substituting Eq. (A.50) into Eq. (A.53) results in

$$E\Delta\eta = 4\sigma_T\{0.5 - [(\sigma_y - \sigma_p)/\sigma_T)]^{1/2}\} \tag{A.54}$$

Ratcheting occurs when the quantity $E\Delta\eta \ge 0$. Hence, Eq. (A.54) becomes

$$(\sigma_p + \sigma_T/4) \ge \sigma_y \tag{A.55a}$$

or

$$X + Y/4 \ge 1.0 \tag{A.55b}$$

The second requirement is that σ_2 in Eq. (A.40) must be greater than $-\sigma_y$ at $z = t/2$. Similarly, σ_3 in Eq. (A.48) must be greater than $-\sigma_y$ at $z = -t/2$. Using one of these two equations yields

$$\sigma_T(\sigma_y - \sigma_p) \le \sigma_y^2 \tag{A.56a}$$

or

$$Y(1 - X) \le 1.0 \tag{A.56b}$$

The final requirement is that the stress due to pressure, σ_p, must be less than the yield stress

$$\sigma_p \leq \sigma_y \tag{A.57a}$$

or

$$X \leq 1.0 \tag{A.57b}$$

Equations (A.55), (A.56), and (A.57) form the boundary of the zone R_1. It is defined by area *BFH* of the Bree diagram in Fig. A.1.

Zone R_2

Ratcheting is assumed to take place in zone R_2. The main characteristic of this zone is that yielding extends past the midwall of the shell due to yielding at both surfaces of the shell. Thus, shakedown will not take place. The derivation of the equations is very similar to that for zone R_1. The area for zone R_2 is defined by area *FGH* of the Bree diagram in Fig. A.1.

APPENDIX B
CONVERSION TABLE

Multiply	By factor	To get units
bar	14.504	psi
cm	0.3937	inches
inches	25.4	mm
kg	2.205	lb
kg/mm^2	14.22	psi
lb	0.454	kg
MPa	145.03	psi
mm	0.03937	inches
psi	0.06895	bar
psi	0.0704	kg/mm^2
psi	0.006895	MPa
°C	1.8C + 32	°F
°F	(F − 32)/1.8	°C

MPa = MN/m^2 = N/mm^2 = 10 bars.

REFERENCES

American Institute of Steel Construction, 1991, *Manual of Steel Construction-Allowable Stress Design*, ASCE, New York.

American Petroleum Institute, 2000, Fitness-for-Service: API Recommended Practice 579, API, Washington, D.C.

American Society of Mechanical Engineers, 1976, ASME-MPC symposium on Creep-Fatigue Interaction, ASME, New York.

American Society of Mechanical Engineers, 2007, *Boiler and Pressure Vessel Code, Section I, Rules for Construction of Power Boilers*, ASME, New York.

American Society of Mechanical Engineers, 2007, *Boiler and Pressure Vessel Code, Section II, Materials*, ASME, New York.

American Society of Mechanical Engineers, 2007, *Boiler and Pressure Vessel Code, Section III, Rules for Construction of Nuclear Facility Components*, ASME, New York.

American Society of Mechanical Engineers, 2007, *Boiler and Pressure Vessel Code, Section VIII, Rules for Construction of Pressure Vessels*, ASME, New York.

ASME, 2004, American Society of Mechanical Engineers, *Power Piping ASME B31.1*, New York, ASME.

ASME, 2004, American Society of Mechanical Engineers, *Power Piping ASME B31.3*, New York, ASME.

Baker, J., and Heyman, J., 1969, *Plastic Design of Frames*, University of Cambridge Press, Cambridge.

Bannantine, J. A., Comer, J. J., and Handrock, J. L., 1990, *Fundamentals of Metal Fatigue Analysis*, Prentice-Hall, New Jersey.

Becht, C., et al., 1989, "Structural Design for Elevated Temperature Environments — Creep, Ratchet, Fatigue, and Fracture," PVP-163, NY, American Society of Mechanical Engineers.

Beedle, L., 1958, *Plastic Design of Steel Frames*, John Wiley Publishing, New York.

Bernasconi, G., and Piatti, G., 1979, *Creep of Engineering Materials and Structures*, Applied Science Publishers Ltd., London.

Boyle, J. T., and Spence, J., 1983, *Stress Analysis for Creep*, Camelot Press, London.

Bree, J., 1967, "Elastic-Plastic Behaviour of Thin Tubes Subjected to Internal Pressure and Intermittent High-Heat Fluxes with Application to Fast-Nuclear-Reactor Fuel Elements," *Journal of Strain Analysis*, **2**(3), pp. 226–238.

Bree, J., 1968, "Incremental Growth Due to Creep and Plastic Yielding of Thin Tubes Subjected to Internal Pressure and Cyclic Thermal Stresses," *Journal of Strain Analysis*, **3**(2).

Burgreen, D., 1975, *Design Methods for Power Plant Structures*, C. P. Press, New York.

Chen, W. F., and Zheng, H., 1991, *Structural Plasticity*, Springer-Verlag, New York.

Conway, J. B., 1969, *Stress-Rupture Parameters, Origin, Calculations and Use*, Gordon and Breach Science Publishers, New York.

Curran, R. M., 1976, "Symposium on Creep Fatigue Interaction, MPC-3, American Society of Mechanical Engineers," New York.

Den Hartog, J. P., 1987, *Advance Strength of Materials*, Dover Publications, Massachusetts.

Dillon, C. P., 2000, *Unusual Corrosion Problems in the Chemical Industry*, Materials Technology Institute of the Chemical Process Industries, Missouri.

Farr, J. R., and Jawad, M. H., 2006, *Guidebook for the Design of ASME Section VIII Pressure Vessels*, ASME Press, New York.

Faupel, J. H., and Fisher, F. E., 1981, *Engineering Design*, John Wiley, New York.

Finnie, I., and Heller, W., 1959, *Creep of Engineering Materials*, McGraw Hill, New York.

Flugge, W., 1967, *Viscoelasticity*, Blaisdell Publishing Company, Massachusetts.

Frost, N. E., Marsh, K. J., and Pook, L. P., 1974, *Metal Fatigue*, Clarendon Press, Oxford.

Goodall, I. W., 2003, *Reference Stress Methods — Analysing Safety and Design*, Professional Engineering Publishing, London.

Grant, N. J., and Mullendore, A. W., 1965, *Deformation and Fracture at Elevated Temperatures*, MIT Press, Massachusetts.

Hill, R., 1950, *The Mathematical Theory of Plasticity*, Oxford Press, London.

Hoff, N. J., 1958, *High Temperature Effects in Aircraft Structures*, Pergamon, New York.

Hult, J., 1966, *Creep in Engineering Materials*, Blaisdell Publishing Company, Massachusetts.

Hyde, T. H., 1994, *Creep of Materials and Structures*, Mechanical Engineering Publications, London.

Jawad, M. H., 2004, *Design of Plate and Shell Structures*, ASME Press, New York.

Jawad, M. H., and Farr, J. R., 1989, *Structural Analysis and Design of Process Equipment*, John Wiley, New York.

Jetter, R. I., 2002, *Companion Guide to the ASME Boiler & Pressure Vessel Code*, Rao, K. R., ed., ASME Press, New York, Volume 1, Chapter 12.

Kraus, H., 1980, *Creep Analysis*, John Wiley Publishing, New York.

Larsson, L. H., 1992, *High Temperature Structural Design*, ESIS 12, Mechanical Engineering Publications, London.

Markl, A., 1960, *Fatigue Tests of Piping Components, Pressure Vessel and Piping Design, Collected Papers, 1927–1959*, ASME, New York.

Neuber, H., 1961, "Theory of Stress Concentration for Shear-Strained Prismatical Bodies With Arbitrary Nonlinear Stress-Strain Law," *ASME Journal of Applied Mechanics*, **28**, pp. 544–550.

O'Donnell, W. J., and Porowski, J., 1974, "Upper Bounds for Accumulated Strains Due to Creep Ratcheting," *Transactions ASME Journal of Pressure Vessel Technology*, **96**, pp. 150–154.

Odqvist, F. K. G., 1966, *Mathematical Theory of Creep and Creep Rupture*, Oxford Mathematical Monographs, Oxford.

Penny, R. K., and Marriott, D. L., 1995, *Design for Creep*, Chapman and Hall, New York.

Prager, M., 1995, "Development of the MPC Omega Method for Life Assessment in the Creep Range," *Journal of Pressure Vessel Technology*, **117**, pp. 95–103.

Prager, M., 2000, "The Omega Method - An Engineering Approach to Life Assessment", Journal of Pressure Vessel Technology, Vol. 122, American Society of Mechanical Engineers, New York.

Rabotnov, Yu. N., 1969, *Creep Problems in Structural Members*, Elsevier, New York.

Rao, K. R., 2002, *Companion Guide to the ASME Boiler and Pressure Vessel Code*, ASME, New York.

Severud, L. K., 1975, "Simplified Methods and Application to Preliminary Design of Piping for Elevated Temperature Service," ASME 2nd National congress on pressure vessels and piping, San Francisco, ASME.

Severud, L. K., 1980, "Experience With Simplified Inelastic Analysis of Piping Designed for Elevated Temperature Services," *ASME Journal of Nuclear Engineering*, ASME, New York.

Severud, L. K., 1991, "Creep-Fatigue Assessment Methods Using Elastic Analysis Results and Adjustments," *ASME Journal of Pressure Vessel Technology*, **114**, pp. 34–40.

Severud, L. K., and Winkel, B. V., 1987, "Elastic Creep-Fatigue Evaluation for ASME Code," Transactions of the 9th International conference on structural mechanics in reactor technology, Lausanne, Switzerland.

Sim, R. G., 1968, "Creep of structures," Ph.D. dissertation, University of Cambridge, Cambridge, U.K.

Smith, A. I., and Nicolson, A. M., 1971, *Advances in Creep Design*, John Wiley, New York.

Sturm, R. G., 1941, "A Study of the Collapsing Pressure of Thin-Walled Cylinders," University of Illinois Engineering Experiment Station Bulletin 329, Urbana, Illinois.

Thielsch, H., 1977, *Defect and Failures in Pressure Vessels and Piping*, Robert E. Krieger Publishing, New York.

Von Karman, T., and Tsien, H., 1960, "The Buckling of Spherical Shells by External Pressure," *Pressure Vessel and Piping Design — Collected Papers 1927–1959*, ASME, New York.

Wang, C. K., 1970, *Matrix Methods of Structural Analysis*, International Textbook Company, Pennsylvania.

Weaver, W., and Gere, J., 1990, *Matrix Structural Analysis*, Van Nostrand, New York.

Wilshire, B., and Owen, D. R. J., 1983, *Engineering Approaches to High Temperature Design*, Pineridge Press, Swansea, U.K.

Winston, B., Burrows, R., Michel, R., and Rankin, A.W., 1954. A Wall-Thickness Formula for High-Pressure Piping, Transactions of ASME, New York.